Biol. Cybern. 90, 51–58 (2004)
DOI 10.1007/s00422-003-0446-2

Biological Cybernetics

Stability in legged locomotion

Tomaž Karčnik

University of Ljubljana, Faculty of Electrical Engineering, Tržaška 25, 1000 Ljubljana, Slovenia

Received: 18 December 2002 / Accepted: 24 September 2003 / Published online: 20 January 2004

Abstract. Stability is a key element in a gait synthesis. Static stability margins are widely adopted in crawlers, while no similar approach has been developed for dynamically stable systems. Utilizing an analytical approach, we developed a set of easy-to-calculate stability indices to describe instantaneous static and dynamic (In)stability for a certain group of walking systems. The analysis is based on a thorough analysis of the interaction between ground reaction forces and the walking system. The indices are applicable to walking systems regardless of the number of legs or mechanical/biological design. We show that static and dynamic stability are independent of each other. We suggest a possible categorization of gait modes based on stability. Stability characteristics are analyzed in a healthy and highly pathological human gait. Finally, we discuss the applicability of the proposed methods.

1 Introduction

A growing interest in walking systems has been encouraged by advances in recent years. One of the key elements in the progress is stability control. In that regard, walking systems are typically divided into two distinct groups:

– Systems utilizing static stability – so-called crawlers,
– Dynamically stable systems.

The systems in the first group usually have at least four legs and walk in such a way that there are at least three feet on the ground at any time (McGhee and Frank 1968). Some bipeds with finite foot-floor contact size can also exercise such gait under certain conditions. The feet in contact with the ground provide a stable base of support for slow movements what is easily observed in animals (Alexander 1983). Three important advantages of such gait mode are gait pattern ensured stability, kinematics/statics based control system and precise trajectory planning/generation. The main drawbacks are energy inefficiency (McGeer 1990) and low velocity.

A plethora of stability indices/margins has been developed so far to describe the degree of static stability:

– Front, rear, side, and overall stability margin (McGhee and Frank 1968), $S_{m,f}$, $S_{m,r}$, $S_{m,s}$, and S_m, describe absolute horizontal distances from the center of gravity to the front, rear, side, or closest supporting area boundaries, respectively.
– Front and rear body-longitudinal stability margins (Zhang and Song 1990) $S_{b,f}$ and $S_{b,r}$, where the distances to the supporting area boundaries are measured along the walking system longitudinal axis.
– Front and rear longitudinal stability margins (Song and Waldron 1989) $S_{l,f}$ and $S_{l,r}$ are the horizontal distances to the front and rear supporting area boundaries as measured in the instantaneous direction of motion. The minimum of the two is known as the longitudinal stability margin S_l.

The longitudinal stability margins are also known as crab stability margins (Zhang and Song 1990). Yet another alternative approach to faster but still statically stable gaits is to use the zero moment point instead of center of gravity as the reference point (Vukobratovic et al. 1990); in this case limited information on the dynamics is included. All these criteria describe the *instantaneous* state of the legged system and not the average or statistical values of the gait, as is usually done in kinesiology (Mayagoitia et al. 1996).

Stability is even more important in a truly dynamically stable gait when the velocity and the kinetic energy are decisive determinants of system behavior. It is due to stability thus a dynamically balanced system can tolerate departures from static equilibrium. The locomotion assures, besides movement of the system from the initial to the final point in space, system stability. If locomotion is interrupted, the machine tips over or falls (Raibert 1986).

Correspondence to: T. Karčnik
(e-mail: karcnikt@robo.fe.uni-lj.si)

Several techniques were developed to quantitatively describe the dynamic stability of walking/running systems.

(Nagy et al. 1994) extended the concept of static stability by calculating the necessary energy to tip over a system using a pseudostatic approach. (Lin and Song 1993) defined the dynamic stability margin as the minimum resulting moment around the boundaries of the supporting polygon normalized to the body weight. (Yoneda et al. 1996) utilized a zero-moment point based dynamic stability assessment. (Hurmuzlu and Basdogan 1994) used phase portraits and Poincare's maps to characterize dynamic stability. Similar techniques were also used by (Koditschek and Bühler 1991) and (Vakakis et al. 1991), who analyzed the stability of the Raibert's one-legged hopping robot. (Berkemeier 1998) analyzed the stability of a 2 DOF model of a quadrupedal gait with a simplified control strategy. Yet another approach (Kimura et al. 1990, Miura and Shimoyama 1984) used a simple inverted pendulum model to deal with system dynamics. A similar approach was also used by (Raibert 1986). Some work has also been done on stability analysis of passive walking systems (Garcia et al. 1998) similar to those developed by (McGeer 1990). Similarly, the group from Waseda University has also used various stability criteria for control of their robots (Yamaguchi et al. 1993). The main drawback of all these contributions is either an extremely simplified model of locomotion in order for Ljapunov/Poincare methods to be applied, or the stability analysis has been performed for a specific type of walking machine, e.g., Raibert's one-legged hopping robot. However, there has thus far been no approach developed for dynamically stable gait that would resemble the idea of static stability margin.

Therefore, we have developed an analytical method to define and calculate an *instantaneous* dynamic stability index. The proposed index, analogous to the static stability margin, answers the fundamental question of whether the walking system is in a dynamically (un)stable state. The results are applicable to any gait mode and any walking system regardless of its degrees of freedom or number of segments due to the very simple end result. Detailed modeling of the walking system is also not necessary. The analysis is first limited to systems where no up/down movement occurs and is later expanded to include other groups. Unlike (Kumar and Waldron 1990), we are not interested in analyzing stability through forces generated by individual legs, an issue very important for static crawlers. The interaction force field and its distribution is thus of no interest to us. We deal only with the net ground reaction force/moment that is the net effect of forces/moments generated by all legs. Also, we do not assume massless legs and zero moment contact between legs and the ground.

2 Terminology and definitions

The entire analysis is performed for walking on a hard, level surface without slipping. A fixed, inertial coordinate system is used for analysis; its origin is situation dependent. The z-axis always points upwards, and the x-axis indicates the average gait direction. The plane $z = 0$ corresponds to the ground plane. We assume the walking system is built of rigid segments and is therefore modeled as a multi segment system.

Gait-related definitions are based on the work of (McGhee and Frank 1968) and (Song and Waldron 1989), with a few extras added, as shown in Fig. 1. The *vertical* projection of COG on the ground plane is marked as PCOG. The leading and trailing stability area edges in the direction of the instantaneous velocity are marked as LSE and TSE, respectively. The center of the supporting area (CS) is the midpoint between LSE and TSE. The CS, LSE, and TSE are defined with respect to the instantaneous PCOG position and its velocity.

Ground reaction forces and moments are the only external forces and moments affecting a walking system. They act on each leg in ground contact. The sum of all ground reaction forces and the sum of all moments are called the net ground reaction force $\boldsymbol{F}^G = \left[F_x^G, F_y^G, F_z^G\right]^T$ and the net ground reaction moment $\boldsymbol{T}^G = \left[T_x^G, T_y^G, T_z^G\right]^T$. The origin of the *net ground reaction force* is called *zero moment point* (ZMP) (Vukobratović et al. 1970), or center of pressure (COP) in kinesiology. The ZMP is always inside the supporting area if no adhesive forces exist between the feet and the ground. The acceleration of the COG and the net ground reaction force are related as

$$\begin{bmatrix} F_x^G(t) \\ F_y^G(t) \\ F_z^G(t) \end{bmatrix} = M \begin{bmatrix} \ddot{x}^{\mathrm{COG}}(t) \\ \ddot{y}^{\mathrm{COG}}(t) \\ \ddot{z}^{\mathrm{COG}}(t) \end{bmatrix} + \begin{bmatrix} 0 \\ 0 \\ F_{gz} \end{bmatrix}, \tag{1}$$

where $M = \sum_{i=1}^{k} m_i$, with m_i being the mass of the i-th segment in a k segment system. $F_{gz} = Mg$ denotes the gravitational force. There also exists the inverse transformation:

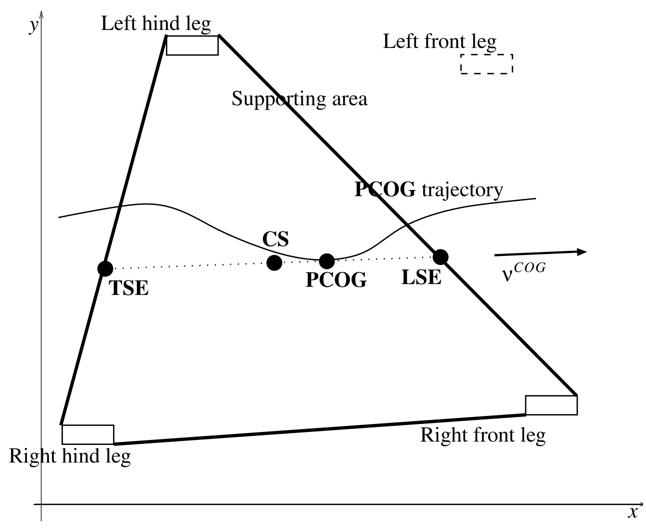

Fig. 1. Top view of a quadruped supporting area with left front leg in swing phase

$$\begin{bmatrix} x^{\mathrm{COG}}(t) \\ y^{\mathrm{COG}}(t) \\ z^{\mathrm{COG}}(t) \end{bmatrix} = \frac{1}{M} \begin{bmatrix} \int_{-\infty}^{t} \int_{-\infty}^{\tau} F_x^G(\upsilon) d\upsilon d\tau \\ \int_{-\infty}^{t} \int_{-\infty}^{\tau} F_y^G(\upsilon) d\upsilon d\tau \\ \int_{-\infty}^{t} \int_{-\infty}^{\tau} F_z^G(\upsilon) - F_{gz} d\upsilon d\tau \end{bmatrix} . \tag{2}$$

We can therefore always calculate the COG trajectory from known net ground reaction forces and vice versa.

When rotational effects are neglected, $\boldsymbol{F}^G$ points from the ZMP precisely to the COG. In the opposite case (1) and (2) are still valid, yet they still describe only the trajectory of the COG. So a pure rotational movement may occur that does not affect either the COG or $\boldsymbol{F}^G$, e.g, rotation around the vertical pitch axis. Obviously, rotations may occur around any axis. The resulting moment is then a 3D vector with mutually independent components.

When rotational effects are taken into account, $\boldsymbol{F}^G$ does not necessarily point to the COG. This results in the moment around the COG:

$$\boldsymbol{T}^F = \left(\boldsymbol{r}^{\mathrm{COG}} - \boldsymbol{r}^{\mathrm{ZMP}}\right) \times \boldsymbol{F}^G . \tag{3}$$

$\boldsymbol{r}^{\mathrm{COG}}$ and $\boldsymbol{r}^{\mathrm{ZMP}}$ denote the position vectors of the COG and the ZMP, respectively. The moment generated in such a way has, in general, three components. However, the moment is the result of only two independent parameters, r_x^{ZMP} and r_y^{ZMP}, while r_z^{ZMP} is zero.

However, a pure ground reaction moment T_z^G also exists: $\boldsymbol{T}^G = \left[0, 0, T_z^G\right]^T$. This moment is the result of the force pairs acting tangentially on the ground plane, resulting in a rotation around the vertical pitch axis. By contrast, there is no moment generated between the feet and the ground around the x- and y-axes. The total moment $\boldsymbol{T}^{\mathrm{COG}}$ is the sum of $\boldsymbol{T}^F$ and $\boldsymbol{T}^G$:

$$\boldsymbol{T}^{\mathrm{COG}} = \boldsymbol{T}^F + \boldsymbol{T}^G = (\boldsymbol{r}^{\mathrm{COG}} - \boldsymbol{r}^{\mathrm{ZMP}}) \times \boldsymbol{F}^G + \begin{bmatrix} 0 \\ 0 \\ T_z^G \end{bmatrix} . \tag{4}$$

Such a $\boldsymbol{T}^{\mathrm{COG}}$ enables a rotation around an arbitrary axis. Because (4) represents a set of three linear equations, it is possible to calculate $\boldsymbol{T}^{\mathrm{COG}}$ from r_x^{ZMP}, r_y^{ZMP}, and T_z^G or vice versa. The actual rotational movement and $\boldsymbol{T}^{\mathrm{COG}}$ are related by

$$\boldsymbol{T}^{\mathrm{COG}} = \frac{d\mathbf{J}\omega}{dt} = \dot{\mathbf{J}}\omega + \mathbf{J}\dot{\omega} , \tag{5}$$

where $\mathbf{J}$ denotes the walking system inertia tensor and ω is a vector of angular velocities.

Using (1), (4), and (5), it is possible to calculate $\boldsymbol{F}^G$ and $\boldsymbol{T}^G$ in a unique way when the system movement is known. Contrary, it is not possible to calculate the system movement when only $\boldsymbol{F}^G$ and $\boldsymbol{T}^G$ are known. In a multisegment system such as walking machines or biological systems, the transformation between $\boldsymbol{T}^{\mathrm{COG}}$ and body movement is not unique, as explained by (5). *Different* activities can generate the *same* $\boldsymbol{F}^G$ and $\boldsymbol{T}^G$, e.g., the rotation of head or trunk around the z-axis in humans.

3 Stability indices

3.1 Kinematic stability

A severe drawback of the statically stable gait is limited maximal velocity, defined for a regular gait as (Waldron et al. 1984)

$$v_{max} = \frac{R}{t_t}\left(\frac{1 - \beta_{\min}}{\beta_{\min}}\right) = K\left(\frac{1 - \beta_{\min}}{\beta_{\min}}\right) . \tag{6}$$

The stroke pitch R and leg transfer time t_t are parameters defined by the system design, and their ratio can be considered as constant K. The highest possible velocity is achieved when the leg duty cycle β is minimal, being $3/n$ for an n-legged system.

The static stability margins do a good job in assessing the system's stability in gaits with low dynamic contents. In such cases the velocity is low compared to the value v_{max} calculated by (6). With further increased gait velocity statically *unstable* phases do occur, and these cannot be described by standard static stability margins. Thus, referring to Fig. 1, we define the relative kinematic stability index as

$$\mathrm{RKSI}_1 = \frac{p(\mathrm{PCOG}, CS)}{\frac{|p(TSE, LSE)|}{2}} , \tag{7}$$

where p denotes the signed distance between the two points. The distance $p(\mathrm{PCOG}, CS)$ is positive if the PCOG is behind the CS and vice versa. All the points, except PCOG, used in the calculation of RKSI_1 change if the direction of the instantaneous COG velocity changes.

The term kinematic stability emphasizes that limited kinematic data have been included. The system is statically/kinematically stable if $-1 \leq \mathrm{RKSI}_1 \leq 1$, and unstable otherwise. The system stability decreases with increasing absolute value of index RKSI_1 and vice versa. The PCOG is ahead of the supporting area if $\mathrm{RKSI}_1 < -1$ or behind if $\mathrm{RKSI}_1 > 1$.

RKSI_1 can also be expressed in terms of longitudinal stability margins if the system is *in* a statically stable phase:

$$\mathrm{RKSI}_1 = \frac{S_{l,f} + S_{l,r} - 2\min(S_{l,f}, S_{l,r})}{S_{l,f} + S_{l,r}} \cdot \mathrm{sign}\left(\frac{S_{l,f} + S_{l,r}}{2} - S_{l,r}\right) . \tag{8}$$

3.2 Dynamic stability

Our approach to assessing dynamic stability is based on (Raibert 1986). Pursuing his ideas we define:

Definition 1 *The system is in a* dynamically stable *state or phase if it can move into a* statically *stable state with zero final velocity without reshaping the supporting area; otherwise the system is in a dynamically unstable state*.

Dynamic stability as specified above can also be understood as a dynamic resistance to falling or tipping over. However, contrary to (Nagy et al. 1994), we do not treat the walking system in a static manner. In our case, the system kinetic energy and supporting area are the decisive factors for stability assessment.

The walking system is in a dynamically stable phase at a given instant of time if the legs provoked ground reaction forces/moments can stabilize the system in a statically stable position without making additional steps. In a dynamically *stable* phase, leg movement or locomotion is not necessary to assure stability. In a dynamically *unstable* state, some leg action is required to prevent falling or tipping over/back; it is the locomotion that assures stability. As we all know from our everyday experience, the ground reaction force/moment affecting the walking system cannot be arbitrary, and thus it is not always possible to stabilize the walking system.

3.2.1 Translational components in 2D space

First we assume all movement consists only of translations limited to the sagittal plane, which coincides with the gait direction. Figure 2 graphically presents important parameters.

The coordinate system origin is placed in the LSE. The entire walking machine body and all the segments have been replaced by the COG, which is $z^{\mathrm{COG}}(t)$ above the ground level and moves forward in the $-x$ direction. The distance $x^{\mathrm{COG}}(t)$ equals the front longitudinal stability margin $S_{l,f}$ if the PCOG is inside the supporting area. The supporting area boundary is shown with dashed lines. The movement of the system is limited to the $y = 0$ plane, and we neglect all rotational effects.

With regard to Definition 1, we want to find out whether a walking machine is, with respect to its current state, capable of compensating its own kinetic energy through applying appropriate forces/moments on the ground. Thus regaining stability means bringing the PCOG to and keeping it within the supporting area. The instantaneous posture, geometrical parameters, and COG velocity $v^{\mathrm{COG}}(t)$ represent the initial conditions.

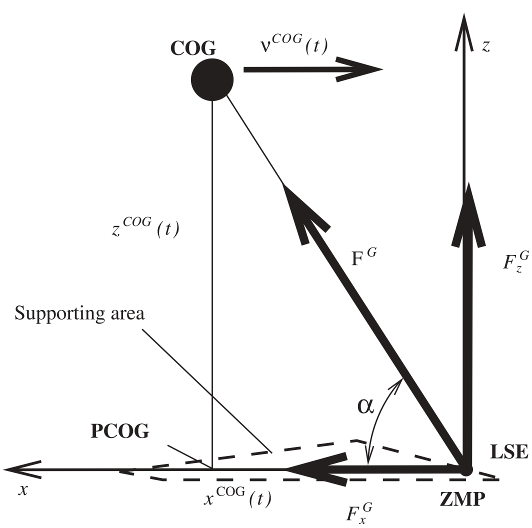

Fig. 2. Calculation of dynamic stability: planar, translation only approach

Compensation can only be achieved through appropriate ground reaction forces, which are the reaction forces to the ones applied to the ground by the walking machine itself and are therefore machine controlled. Obviously, the decisive component for compensating the kinetic energy is the braking force F_x^G, which compensates the system kinetic energy due to the progression in the direction of gait. However, $\boldsymbol{F}^G$ and therefore F_x^G cannot be arbitrary because $\boldsymbol{F}^G$ always points toward the COG and the ZMP is always inside the supporting area. The maximal braking force is achieved if the ZMP is in the LSE, as shown in Fig. 2. It follows that

$$\frac{F_z^G}{F_x^G} = \frac{z^{\mathrm{COG}}(t)}{x^{\mathrm{COG}}(t)} = \tan(\alpha) \ , \tag{9}$$

where $x^{\mathrm{COG}}(t)$ and $z^{\mathrm{COG}}(t)$ are defined by the system posture. Theoretically, an arbitrary braking force F_x^G can be achieved if F_z^G is also increased at the same rate. But F_z^G can be increased only if the appropriate $\ddot{z}^{\mathrm{COG}}$ is generated, as shown by (1). This results in an accelerated vertical rising throughout the braking process, which might become a vertical jump. From a practical point of view the maneuver is unlikely to be performed by a walking machine, though the same phenomenon is, for example, observed to a limited extent in normal human gait termination (Jian et al. 1993). Thus we assume no rising can occur:

Assumption 1 $\ddot{z}^{\mathrm{COG}} = 0$ yields $F_z^G = F_{gz}$.

z^{COG} is no longer time dependent and becomes constant: $z^{\mathrm{COG}}(t) = z^{\mathrm{COG}}(t_0) = z^{\mathrm{COG}}$. The maximum braking force is then simply

$$F_x^G = \frac{x^{\mathrm{COG}}(t)}{z^{\mathrm{COG}}} F_{gz} \ . \tag{10}$$

By applying Assumption 1 and (1) we can rewrite (10) as a linear differential equation with constant coefficients:

$$\ddot{x}^{\mathrm{COG}}(t) - \frac{g}{z^{\mathrm{COG}}} x^{\mathrm{COG}}(t) = 0 \ . \tag{11}$$

Assumption 1 reduces the infinite number of solutions for (11) to a single one. The solution for the initial conditions $x(0) = 0^+$ and $\dot{x}(0) = 0$ is described in the phase plane as

$$v^c(t) = \sqrt{\frac{g}{z^{\mathrm{COG}}}} x^{\mathrm{COG}}(t) \ . \tag{12}$$

The initial conditions describe the most extreme yet statically stable state of a walking system: PCOG is almost at the supporting area boundary, $x(0) = 0^+$ and the COG velocity $v^{\mathrm{COG}}(0)$ is zero, and $\dot{x}(0) = 0$. $v^c(t)$ represents *critical velocity* because it still adheres to Definition 1 for dynamic stability. $v^c(t)$ is therefore the maximal velocity that the system can compensate with respect to the given posture and supporting area geometry without moving its legs.

So far we have considered only the problem of tipping forward. But there also exists the possibility of tipping backward, though it might not be the case that often, e.g., the COG is behind the supporting area while the COG velocity is too low to bring the COG above the supporting area. In such a case, the trailing legs should be moved backward to maintain the balance.

The approach is similar to the one above except that in this case we are looking for minimal F_x^G. The origin of $\boldsymbol{F}^G$ is therefore placed at the trailing stability edge (TSE). Similarly, we derive the *trailing critical velocity* by following the same procedure as above:

$$v_t^c(t) = \sqrt{\frac{g}{z^{\mathrm{COG}}}} x_t^{\mathrm{COG}}(t) \;\;, \tag{13}$$

where $x_t^{\mathrm{COG}}(t)$ is the signed distance from TSE to PCOG. If PCOG is inside the supporting polygon, the trailing critical velocity $v_t^c(t)$ is correctly negative.

We can conclude:

Theorem 1 *Overall, the system is dynamically stable at a given instant of time if and only if*

$$v_t^c(t) \leq v_x^{\mathrm{COG}}(t) \leq v^c(t) \;\; .$$

It turns out that, in real-world applications, comparison with $v^c(t)$ is much more important than with $v_t^c(t)$. Overall, the calculation of dynamic stability is reduced to a comparison between

– actual COG velocity and
– easy-to-determine critical velocities.

For this reason instantaneous dynamic stability can be quantitatively described by the *absolute velocity index*.

Definition 2 *The absolute velocity index* (AVI) *is defined as*

$$\mathrm{AVI} = v^c\big(x^{\mathrm{COG}}(t)\big) - v_x^{\mathrm{COG}}(t) = \sqrt{\frac{g}{z^{\mathrm{COG}}}} x^{\mathrm{COG}}(t) - v_x^{\mathrm{COG}}(t) \;\; . \tag{14}$$

The AVI units are *m/s*, and the index describes the difference between critical and actual velocity. The index equals the dynamic stability margin and is expressed as velocity. The system dynamic (In)stability can be thus expressed in terms of AVI. If AVI is positive, the system is in a dynamically stable state and vice versa. The dynamic stability of the system increases if the index is higher.

Relative indices, which express dynamic stability margins relative to the actual or critical velocities, are also sometimes important.

Definition 3 *The first and second relative velocity indices* (RVI_1 *and* RVI_2) *are defined as:*

$$\mathrm{RVI}_1 = \frac{v_c\big(x^{\mathrm{COG}}(t)\big) - v_x^{\mathrm{COG}}(t)}{v_x^{\mathrm{COG}}(t)} , \tag{15}$$

$$\mathrm{RVI}_2 = \frac{v_c\big(x^{\mathrm{COG}}(t)\big) - v_x^{\mathrm{COG}}(t)}{v_c(x^{\mathrm{COG}}(t))} \;\; . \tag{16}$$

Similarly, we could also define trailing dynamic stability indices, but in practice they are not as important as the ones described above.

Based on the above analysis we can draw some simple conclusions. The system is always in a dynamically *unstable* state if PCOG is ahead of the supporting area. However, there is no such state, assuming $v^{\mathrm{COG}}(t) \neq 0$, that would "a priori" guarantee dynamic stability. The described approach is meaningless if there is no supporting area in the direction of instantaneous COG velocity, e.g., ballistic phase of running. In such cases the system is by default in a dynamically unstable state.

3.2.2 Stability in 3D space

In this case it is not possible to assess the dynamic stability by extending the approach shown above due to the fact that the supporting area can be of arbitrary size and/or shape and thus cannot be described analytically. Also, the ZMP can move around, and there is also no clear "a priori" answer as to where to place it to achieve the best result. We are thus looking for a minimal path S_{min} defined with respect to (2) as

$$\begin{aligned} S_{min} &= \min||\boldsymbol{S}|| \\ &= \min\left|\left|\int_0^t \int_0^\tau \frac{\boldsymbol{F}^G(\upsilon) - \boldsymbol{F}_g}{M} d\upsilon d\tau + \int_0^t \boldsymbol{v}_{\mathrm{COG}}(\tau) d\tau\right|\right| \;, \end{aligned} \tag{17}$$

given that

– $\boldsymbol{v}^{\mathrm{COG}}(t) = 0$,
– the ZMP is always inside the supporting area, and
– the line through PCOG in the direction of instantaneous velocity must pass through the supporting area.

Equation (17) can only be solved on a case-specific basis by numerical and optimization techniques. However, it is still possible to prove the theorem:

Theorem 1 *If a walking system is dynamically stable in the vertical plane parallel to the instantaneous walking direction as given by Theorem 13, then the system is also stable in 3D space.*

Let us consider Fig. 3, which shows the top view of the walking system in a 3D space. The supporting area boundary is indicated by the thick dashed/solid line the relevant part of the supporting area boundary by the solid line. The coordinate system originates in LSE. PCOG moves forward with v_x^{COG} in the $-x$ direction. v_x^{COG} is divided into two components: v_r^{COG} and v_t^{COG}, perpendicular and tangential components to the leading supporting area boundary, respectively. Distance d^{COG} is the distance between PCOG and the leading supporting area boundary, and x^{COG} is the distance from PCOG to the supporting area boundary in the direction

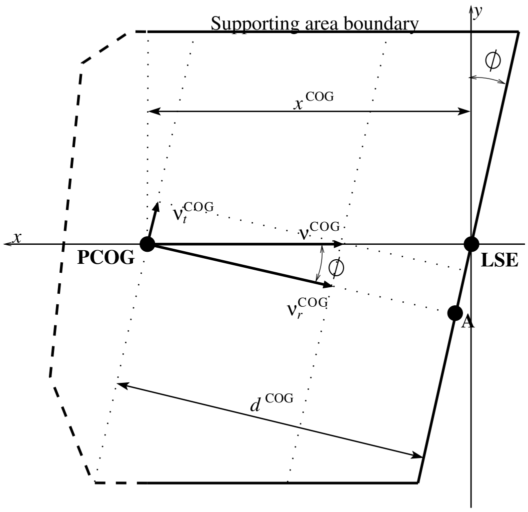

Fig. 3. Top view of supporting area

of the instantaneous PCOG velocity. The leading area boundary is inclined for ϕ to the y-axis.

Suppose that $v_x^{COG}(t) > v^c(t)$ so that the system conforms to Theorem 1 unstably. The critical part is obviously $v_r^{COG}(t) = v_x^{COG}(t)\cos\phi$. Thus the system is in a dynamically stable state if we can compensate $v_r^{COG}(t)$ before PCOG slips out of the supporting area. Analogous to the 2D problem, is the ZMP placed at point A, as marked in Fig. 3. The critical velocity in the direction of the $v_r^{COG}(t)$ is

$$v_r^c(t) = \sqrt{\frac{g}{z^{COG}}} d^{COG}(t) = \sqrt{\frac{g}{z^{COG}}} x^{COG}(t)\cos\phi = v^c(t)\cos\phi \quad . \tag{18}$$

The critical and actual velocities are scaled by the same factor $\cos\phi$, and thus their relative ratio remains the same. Since $v_x^{COG}(t) > v^c(t)$, it also holds that $v_r^{COG}(t) > v_r^c(t)$. The system is unstable in 3D space if it is unstable in 2D space and vice versa, which proves Theorem 2.

3.2.3 Rotational components and dynamic stability.
So far we have neglected the rotational kinetic energy. If rotational components are included in the analysis, we can no longer reduce the movement of the entire walking system to the movement of the COG; the movement of the entire system becomes important.

The analytical approach to the calculation of dynamic stability is no longer possible. Even if we define the optimal ground reaction braking force, it can still result in a variety of possible system motions, as shown in Sect. 2. Additionally, the rotation around the z-axis does not influence the system stability at all, though it shows up as part of system kinetic energy. In this regard, Definition 2 of dynamic stability is no longer valid. Only case-specific numerical optimization techniques can be employed to analyze the dynamic stability of a walking system in this case.

However, we can at least assess the average influence of the rotational components. In a normal healthy human biped gait, the peak ratio between rotational and translational kinetic energy is barely over 0.03 in the mid-leg swing phase (Winter 1979). The average is below 0.02. We can conclude that the error in dynamic stability assessment is in the same range if rotational components are neglected.

The ratio is of course different for nonhumanoid walking robots. The major part of the rotational kinetic energy in the walking machine is the result of leg movement. However, the legs are usually light compared to the robot body, and the resulting error would be even smaller than in human gait.

4 Implications and results

The first conclusion is that static/kinematic and dynamic stability are mutually exclusive: the system can be statically stable but would tip over due to the system dynamics, being therefore dynamically unstable. This is the case when PCOG is close to the leading supporting area edge and v^{COG} is not negligible. The opposite case, a statically unstable but dynamically stable state, can also be found: when PCOG is behind the supporting area and v^{COG} is sufficient to bring the system into a statically stable position.

The classical division of gait modes is thus inappropriate and inaccurate. The suitable gait categorization based on static stability only is as follows: Statically stable: all gait phases are statically *stable*; Semistatically stable: some gait phases are statically *unstable*, others are *stable*; Statically unstable: all gait phases are statically *unstable*.

Similarly, we divide the gait modes in terms of dynamic stability: Not dynamically stable: gait consists of only dynamically *stable* states; Semidynamically stable: gait consists of both dynamically *stable* and *unstable* states; Dynamically stable: gait consists of only dynamically *unstable* states.

For example: normal human gait is semistatically stable but fully dynamically stable.

The control system design depends on stability characteristics:

(1) The kinematic model suffices for gaits consisting of only both statically and dynamically stable states. In this case the movement of the legs dictates the movement of the body. The leg mechanics and control system capabilities determine the velocity of the gait with regard to (6).
(2) When statically unstable states occur while only dynamically stable states are present, the system inertial properties have to be incorporated into the control at the very least. Typically, an inverted pendulum model is sufficient.
(3) In cases where unstable states of both kinds occur, the movement of the body dictates the movement of the legs, which have to keep pace with the movement of the body. In this case the full dynamic model is

built into the control system and has to operate in hard real time.

The control complexity increases with each item but results in higher velocity and generally also better energy efficiency. A typical example is gait rehabilitation in humans after injuries affecting locomotor apparatus (Karčnik and Kralj 1999). Gait rehabilitation usually starts in parallel bars and then proceeds to a walker-assisted gait; both methods provide a large supporting area and good static stability. Next, crutches are used, which enable the introduction of unstable states. Eventually, normal dynamically stable gait might be restored.

To demonstrate the application of stability indices, we performed the stability analysis for two different human gait modes as shown in Figs. 4 and 5. In both cases we present RKSI_1 and AVI describing static/kinematic and dynamic stability, respectively. Stable/unstable regions for each index are specified on the vertical axes. The gait diagram indicates when a particular extremity has been in contact with the ground: thick lines indicate the period of the support phase. The data for the normal gait are taken from (Winter 1979). The methodology and measurement techniques used in the latter case are described in (Karčnik and Kralj 1999).

Figure 4 shows one period of a free, healthy, biped human gait. We clearly see that most of the time the subject was in a statically stable state, when $|\mathrm{RKSI}_1| < 1$. The statically unstable states were of both kinds: with the COG ahead of the supporting area ($0.45 \leq t \leq 0.49$) and the COG behind the supporting area ($0.06 \leq t \leq 0.15$). In the former case $\mathrm{RKSI}_1 > 1$, and in the latter case $\mathrm{RKSI}_1 < -1$. AVI shows that only dynamically unstable states occurred throughout the gait cycle. The abrupt changes in both indices occur due to the heel-off and foot-flat events.

Figure 5 presents an extreme case: a crutch-assisted exercise level gait of a complete spinal cord injured subject (SCI) that exercised a low-speed reciprocal crawl gait pattern with the help of functional electrical stimulation (Kralj and Bajd 1989). Kinematically, crutch-assisted gait is a quadrupedal gait. The gait diagram clearly indicates that only one extremity at a time is in a swing phase. Even more, the subject is always in both

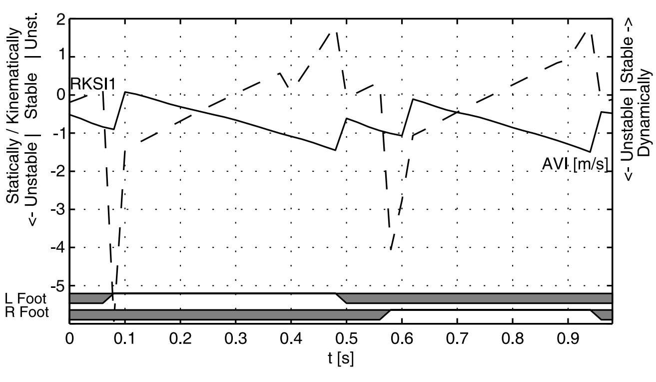

Fig. 4. One complete gait cycle of a free human gait consists of dynamically *unstable* and statically *stable and unstable* states

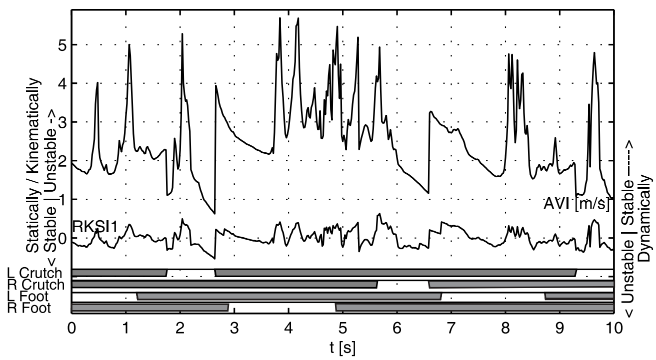

Fig. 5. Crutch-assisted SCI subject gait utilizes only statically and dynamically *stable* states

statically and dynamically stable state. RKSI_1 is close to 0, which indicates that PCOG moves only slightly around the center of the supporting area. AVI is always clearly positive, indicating that only dynamically stable states occurred. This gait is still much too slow to become a dynamics-driven one. It is categorized as a statically stable and nondynamically stable gait.

The final question is how to use various indices. It is clear that static stability margins suffice for statically and nondynamically stable gait. For safety reasons, their usage is further restricted to cases where PCOG is inside the conservative supporting area (Nagy et al. 1994). RKSI_1 can be used when PCOG comes close to the supporting area boundary or when the gait is statically semistable but still nondynamically stable. When gait becomes at least semidynamically stable, the dynamic stability indices must be used. The difference between RVI_1 and RVI_2 becomes important if the denominator in either case becomes small, resulting in a high value of either index. The two should therefore be used in tandem. Furthermore, at near zero velocities $v^{\mathrm{COG}}(t) \rightarrow 0$, (14) yields $\mathrm{AVI} = S_{l,f}\sqrt{g/z^{\mathrm{COG}}(t)}$, meaning that AVI is then just a scaled longitudinal static stability margin. The index AVI is therefore most universally applicable.

5 Conclusion

The proposed set of indices successfully describes all walking machines regardless of the gait pattern utilized. The stability indices can be easily calculated and are particularly suitable for transitions between gait patterns. Their main advantages are that they indicate whether or not a system is instantaneously stable and they eliminate the need for detailed modeling. By contrast, Ljapunov's or Poincare's methods require either development of an (overly) simplified model or execution of several gait cycles before stability assessment can be performed.

An interesting question concerns the required static friction coefficient $\mu = F_x^G(t)/F_z^G(t)$ for propulsion/braking forces used in the dynamic stability assessment. We know from our own experience that low friction dramatically reduces system stability, e.g, the banana peel effect or icy walkway. For example, the human gait, at standard gait parameters (Winter 1979) step length 0.75 m and $z^{COG} = 1.05$ m, results in the highest required $\mu \geq \frac{0.75/2}{1.05} = 0.36$. In human walking it is almost always the case that rubber-soled shoes provide $\mu > 0.6$, even on a wet surface. The critical value of μ depends, of course, on system configuration, but in the case of rubber leg tips the friction coefficient is not likely to be the limiting factor in any walking system.

The most important drawback of the described approach is given by Assumption 1. It is highly unlikely that this assumption is strictly upheld in practice. Unfortunately, the conversion between kinetic and potential energy can be the decisive factor. In human gait, when we try to stop abruptly, we rise slightly on our toes, thus converting part of a system's inertia or kinetic energy into potential energy (Jian et al. 1993). Thus only part of actual kinetic energy has to be compensated. If we were able to increase COG for $h = 10$ cm, we would compensate $v = \sqrt{2gh} = \sqrt{2}m/s$, which is the average velocity of a free human gait. However, that would require extreme forces on the leading legs.

On the other hand, we can rather easily extend the above approach to allow various types of vertical movement forbidden so far by Assumption 1. Let us, for example, apply the same simple criterion as above: $\max\left|\triangle z^{COG}\right| < h$; in other words, the COG can increase or decrease for up to h during the stabilization process. The maximal amount of kinetic energy transformed into/from potential energy equals Mgh. Thus the critical velocities $v^c(t)$, $v_t^c(t)$ as defined in (12), (13), and Theorem 13 are adjusted up and down, respectively, for $v_a = \pm\sqrt{2gh}$. Such a system has, as expected, larger dynamic stability margins. Various other limitations can be placed on $z^{COG}(t)$ and/or its derived quantities, which may describe the actual walking system in a more accurate way.

It is also clear that (11) is actually a model of an inverted pendulum. The kinetic energy compensated through braking and following Assumption 1 is the *same* as it would be if it were converted to potential energy in the inverted pendulum case. In general the behavior of the walking systems is somewhere in between and we can thus consider Assumption 1 fulfilled. Additionally, such a "raising" maneuver is usually not included in the robot controller.

We might also speculate that if the system behavior is close to the inverted pendulum, the system exhibits good energy efficiency. The pendulum is, theoretically, an ideal device with no energy dissipation. The problem, however, is how to efficiently transfer the support from one leg to another. Obviously, systems with dynamically stable gait adhere better to the inverted pendulum model. We may speculate that (11) offers a simple explanation of why we can anticipate better energy efficiency in dynamically stable walkers compared to the static crawlers.

Acknowledgements. The author acknowledges the Republic of Slovenia Ministry of Education, Science, and Sports for financial support and Professor Miloš Žefran for many valuable comments.

References

Alexander R (1983) A dynamic similarity hypothesis for the gaits of quadrupedal mammals. J Zool Lond 201: 135–152

Berkemeier MD (1998) Modeling the dynamics of quadrupedal running. Int J Robot Res 17(9): 971–985

Garcia M, Chatterjee A, Ruina A, Coleman M (1998) The simplest walking model: stability, complexity and scaling. Trans ASME J Biomech Eng 120(2): 281–288

Hurmuzlu Y, Basdogan C (1994) On the measurement of dynamic stability of human locomotion. Trans ASME J Biomech Eng 116: 30–36

Jian Y, Winter D, Ishac M, Gilchrist L (1993) Trajectory of the body COG and COP during the initiation and termination of gait. Gait Posture 1: 9–22

Karčnik T, Kralj A (1999) Stability and velocity in incomplete SCI subjects gait. Artif Org 23(5): 421–423

Kimura H, Shimoyama I, Miura H (1990) Dynamics in the dynamic walk of a quadruped robot. Adv Robot 4(3): 283–301

Koditschek DE, Bühler M (1991) Analysis of a simlified hopping robot. Int J Robot Res 10(6): 587–605

Kralj A, Bajd T (1989) Functional electrical stimulation: standing and walking after spinal cord injury. CRC Press, Boca Raton, FL

Kumar V, Waldron K (1990) Force distribution in walking vechicles. Trans ASME J Mech Des 112: 90–99

Lin BS, Song S (1993) Dynamic modeling, stability and energy efficiency of a quadrupedal walking machine. In: Proceedings of the IEEE conference on robotics and automation, Atlanta, GA, day month 1993, pp 367–373

Mayagoitia R, Lotters J, Veltink P (1996) Standing stability evaluation using a triaxial accelerometer. In: Proceedings of the 18th IEEE conference on engineering in medicine and biology, Amsterdam, day month 1996, p 856

McGhee R, Frank A (1968) On the stability properties of quadruped creeping gaits. Math Biosci 3: 331–351

McGeer T (1990) Passive dynamic walking. Int J Robot Res 9(2): 62–82

Miura H, Shimoyama I (1984) Dynamic walk of a biped. Int J Robot Res 3(2): 60–74

Nagy P, Desa S, Whittaker W (1994) Energy-based stability measures for reliable locomotion of statically stable walkers: theory and application. Int J Robot Res 13(4): 272–287

Raibert MH (1986) Legged robots that balance. MIT Press, Cambridge, MA

Song S-M, Waldron KJ (1989) Machines that walk: adaptive suspension vehicle. MIT Press, Cambridge, MA

Vakakis A, Burdick J, Caughey T (1991) An "interesting" strange attractor in the dynamics of a hopping robot. Int J Robot Res 10(6): 606–618

Vukobratovic M, Borovac B, Surla D, Stokić D (1990) BIPED locomotion: dynamics, stability, control and application. Springer, Berlin Heidelberg New York

Vukobratović M, Frank A, Juričić D (1970) On the stability of biped locomotion. IEEE Trans Biomed Eng BME-17(1): 25–36

Waldron K, Vohnout V, Perry A, McGhee R (1984) Configuration design of the adaptive suspension vehicle. Int J Robot Res 3(2): 37–48

Winter D (1979) Biomechanics of human movement. Wiley, New York

Yamaguchi J, Takanishi A, Kato I (1993) Development of biped walking robot: compensating for three-axis moment by trunk motion. In: Proceedings of IROS' 93, location, day month 1993, pp 561–566

Yoneda K, Iiyama H, Hirose S (1996) Intermittent trot gait of a qadruped walking machine dynamic stability control of an omnidiretcional walk. In: Proceedings of the IEEE international conference on robotics and automation, Minneapolis, day month 1996, pp 3002–3007

Zhang C, Song S-M (1990) Stability analysis of wave-crab gaits of a quadruped. J Robot Sys 7(2): 243–276